On-Wafer, Cryogenic Characterization of Ultra-Low Noise HEMT Devices

J. J. Bautista
Radio Frequency and Microwave Subsystems Section

J. Laskar
University of Hawaii, Honolulu

P. Szydlik
State University of New York, Plattsburgh

Significant advances in the development of high electron-mobility field-effect transistors (HEMTs) have resulted in cryogenic, low-noise amplifiers (LNAs) whose noise temperatures are within an order of magnitude of the quantum noise limit (hf/k). Further advances in HEMT technology at cryogenic temperatures may eventually lead to the replacement of maser and superconducting–insulator–superconducting front ends in the 1- to 100-GHz frequency band. Key to identification of the best HEMTs and optimization of cryogenic LNAs are accurate and repeatable device measurements at cryogenic temperatures. This article describes the design and operation of a cryogenic coplanar waveguide probe system for the characterization and modeling of advanced semiconductor transistors at cryogenic temperatures. Results on advanced HEMT devices are presented to illustrate the utility of the measurement system.

I. Introduction

The noise and gain of high electron-mobility field-effect transistor (HEMT) devices have steadily improved as the technology is being developed and commercialized worldwide for room temperature applications. Although device noise temperatures continue to drop at room temperature, there is no guarantee that the same improvements will occur at cryogenic temperatures. In order to successfully develop ultra-low noise HEMTs for cryogenic applications, one must have quick, accurate, and repeatable cryogenic data and a good device model.

The cryogenic on-wafer noise and scattering parameter measurement system under development is key to the systematic investigation of the dc and microwave properties of advanced HEMT devices. The measured parameters are required to evaluate and verify room temperature and cryogenic device models for the identification of the optimum cryogenic HEMT structure. The measured parameters along with the device models are also needed to design and optimize input, interstage, and output matching circuits for multiple-stage HEMT low-noise amplifiers (LNAs).

A cryogenic study and an empirical model for the cryogenic operation of an advanced pseudomorphic HEMT (PHEMT) device are presented. The original apparatus for making these measurements and the

new system currently under development are described. The methods for making accurate, high-frequency variable temperature scattering (45-MHz to 40-GHz) and noise parameter (2-to 18-GHz) measurements from 11 to 300 K are discussed. Details of the experimental technique, including calibration considerations, are also presented.

II. Cryo-Probe Measurement System

Over the past several years, the development of a complete on-wafer cryogenic microwave measurement system has been primarily driven by the need for (1) greater understanding of the device physics in advanced high-speed transistor technologies, (2) continued advancement of cryogenic LNAs with noise temperatures less than five times the quantum limit ($T_n < 5hf/k$) for ground and space-based applications, and (3) hybrid and monolithic microwave integrated-circuit (MMIC) semiconductor–superconductor circuits.

In 1976, Liechti and Larrick [1] designed a microwave test fixture that could be immersed in liquid nitrogen. Similar types of setups have been used [2–7] to evaluate HEMT performance from 300 to 15 K. To date, it has been difficult to make broadband scattering (S)-parameter measurements in such an environment, due to the limited accuracy of the full two-port calibrations.

The cryogenic microwave system in this work uses coplanar waveguide probes in a vacuum station coupled to a vector network analyzer for scattering parameter measurements, and a noise meter and noise test set with a noise system for microwave noise parameter measurements. The microwave measurement system currently under development, schematically shown in Fig. 1(a), incorporates measurement tools originally developed for the first system in 1989 [8,9]. The cryogenic probe measurement system, shown in Fig. 1(b), contains ports for RF cables, thermometers, vacuum pumps, dry nitrogen back-fill lines, coplanar probes with manipulators, and a closed-cycle refrigerator cold head. The probe body, shown in Fig. 1(c), rests on a copper block attached to a fiberglass post. The fiberglass reduces the thermal load, and copper braiding from the cold head thermally anchors the probe to the 12-K cold station, assuring sample temperatures of 12 to 20 K. The mechanical and thermal stability of the wafer stage is established by supporting it on fiberglass posts above the cold head and thermally anchoring it to the cold station with flexible copper braids.

The most important feature of this design is the incorporation of a closed-cycle helium refrigeration system. The first successful designs of on-wafer cryogenic systems used open-cycle cooling to reduce start-up costs and avoid mechanical vibrations. However, for long term use at the rate of one cool down per week, a closed-cycle system is significantly less expensive. In fact, after the first 6 months of operation, the savings in liquid helium is comparable to the price of a the closed-cycle refrigerator. Decoupling and damping of the vibrations from the cold head to the probe station are accomplished with a two-dimensional bellows and vibration mounts, shown in Fig. 1(b). This system allows small-signal microwave measurements from dc to 40 GHz over a physical temperature range of 16 to 300 K. Since the microwave hardware is insulated by vacuum, there are no frost buildup or large thermal gradients, resulting in a system that is accurate, reliable, and flexible (active and passive discrete devices as well as MMICs can be measured).

III. Calibration and Measurement Considerations

The key to accurate on-wafer microwave and millimeter-wave measurements is proper establishment of the electrical reference plane. The reference plane can be determined with either the line-reflect-match (LRM) or the short-open-load-thru (SOLT) calibration method using an impedance standard substrate (ISS) available from Cascade Microtech [10]. The LRM method requires fewer standards, and the reflect standards need not be well known. In addition, experience has shown that the LRM calibration is slightly better in accuracy than is the SOLT at cryogenic temperatures. In the SOLT method, the short standard

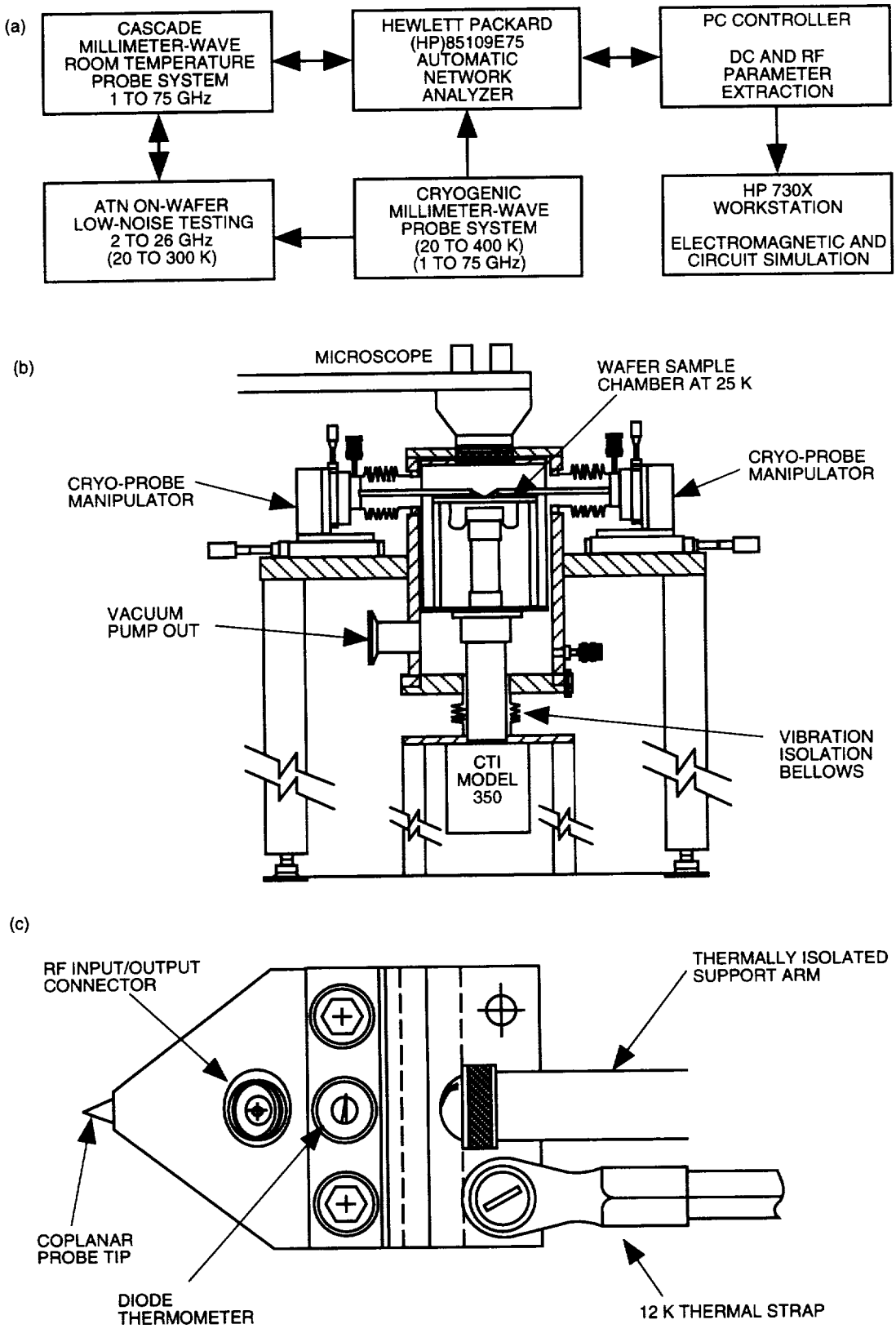

Fig. 1. Cryo-probe (a) measurement system, (b) system, and (c) tip.

introduces uncertainty in the reference plane location because of sensitivity to probe tip placement. The LRM method obviates this problem by replacing the short with an open and by having the probe tip held approximately 10 mils above the substrate during the calibration sequence.

The measurement accuracy is also directly related to the calibration conditions. Thermal gradients across the gold-plated ceramic probe tips and coax to coplanar transitions [11] alter the electrical characteristics of the measurement lines. The process of cooling the sample in the laboratory can also produce changes in the calibration. The network analyzer typically requires a new calibration if the ambient laboratory temperature varies by greater than ± 1 deg C. The proximity of the cooled probe system to the network analyzer can change the ambient environment (both temperature and humidity). The combined results of these effects are appreciable errors in cryogenic temperature measurements. For example, room temperature calibrations have been shown to introduce as much as a 20-percent [8] error in the cryogenic measurement. In addition, measured results have been reported with room temperature calibrations with moding effects [11,12] and deviations from one-pole roll-off [4,11].

Since the microwave probe offers a significant thermal load to the device under test, it is evident that the chuck and device temperatures are different. For example, with a chuck temperature of 20 K and the probes contacting the device under test (DUT), a DUT temperature as high as 50 K has been observed. This large temperature differential affects calibration and skews the interpretation of data collected at different device temperatures.

The solution to maintaining calibration integrity and achieving low sample temperatures is to thermally anchor the probe body and perform cryogenic calibrations. By thermally anchoring the probe to the cold head at 12 K, the thermal load to the DUT is minimized. The remaining microwave hardware [connectors, cables, and input to the automatic network analyzer (ANA)] are thermally isolated via vacuum and stainless steel hardware. The thermally anchored probe can be calibrated at specific temperatures during a measurement cycle. This eliminates the problem of moding (deviation from one-pole roll-off) and allows accurate correlation of DUT temperature and measured characteristics. The S-parameter data shown in Fig. 2 are an example of data collected in this manner.

A reliable cryogenic, two-port calibration for S-parameter measurements must satisfy several criteria. The return loss of the transmission through standard should be better than −45 dB, and the insertion loss should vary within ±0.1 dB of 0 dB. Next, the calibrated open standard, as noted in the previous paragraph, should also be within ±0.1 dB of 0 dB, as shown in Fig. 3. A more extensive verification can be performed by evaluating additional representative elements not used in the calibration sequence. These measurements may include the reflection from a coplanar transmission line (open circuit stub) and a 10-dB pad. The input and output scattering parameters of the open circuit stub should be concentric spirals on the Smith Chart, with a magnitude of less than 1 and the insertion loss of the pad within ±2 percent of 10 dB.

The most accurate and repeatable method of measuring noise parameters at cryogenic temperatures is to place the impedance generator within a wavelength of the DUT input. The equivalent noise temperature of the noise source must also be comparable to the DUT noise temperature. This approach would, however, require development of a cryogenic noise generator and noise source.

For this initial investigation of on-wafer noise parameter measurements at cryogenic temperatures, only the probe tips are cooled while the impedance state generator and solid-state noise source (both commercially available) are kept at room temperature (several wavelengths away from the DUT). In this configuration, the input losses introduce noise comparable to or greater than the noise of the device under test (DUT) and reduce the range of available impedance states. For example, in the frequency range of 2 to 18 GHz for cryogenic temperatures, the worst-case noise temperature error is ±25 K, while device noise temperatures are typically under 10 K. Although this configuration does not provide accurate single-frequency noise parameter measurements, it does provide for fast and efficient broadband

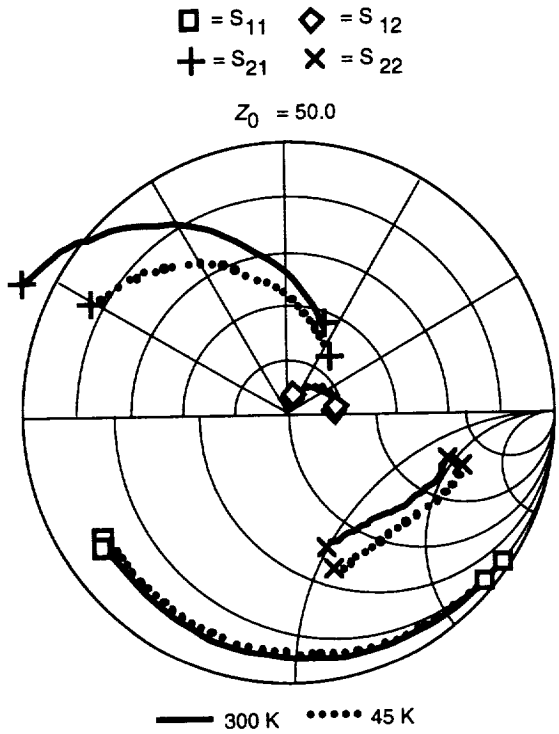

Fig. 2. Cryo-probe measured scattering parameters of an HEMT device at 300 and 45 K from 2 to 20 GHz.

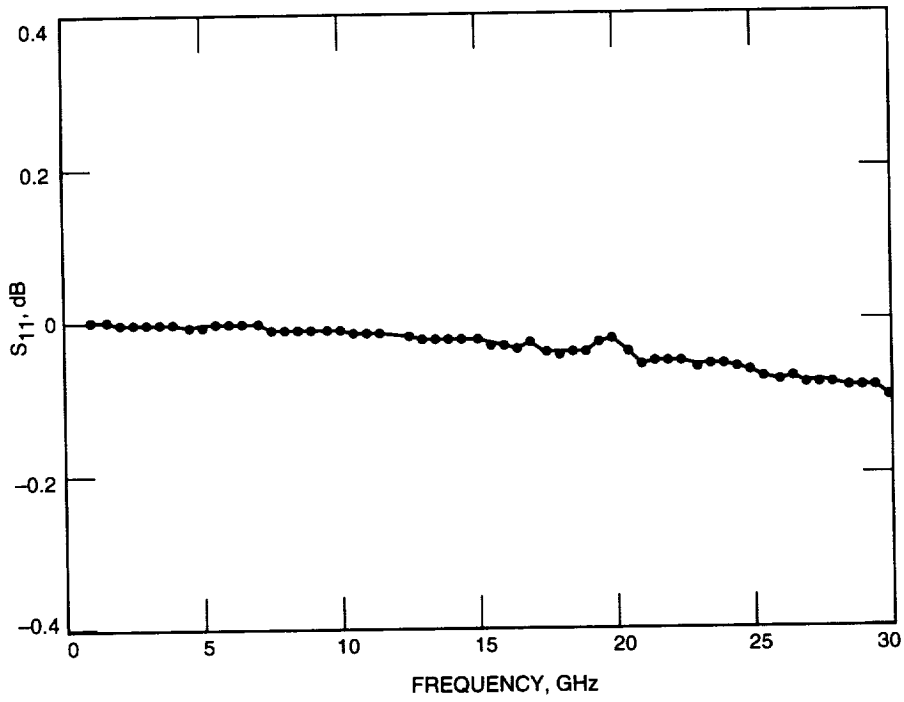

Fig. 3. Variation in open standard at a physical temperature of 20 K using LRM calibration.

(2- to 18-GHz) on-wafer measurements. The noise calibration must pass all the S-parameter calibration criteria and accurately measure the minimum noise temperature (T_m) and associated gain (G_A) of a 10-dB attenuator. An example of the insertion loss of a 10-dB attenuator is shown in Fig. 4. For the noise calibration, the T_m and G_A should be repeatable to within ± 5 percent for the attenuator at a variety of temperatures.

IV. Small-Signal Modeling

A detailed knowledge of the HEMT small-signal equivalent circuit is necessary for designing high-speed circuits and low-noise amplifiers and for understanding the device physics. There are three main methods for small signal parameter extraction: (1) complete parameter extraction from calculations on the measured S-parameters [13], (2) parameter extraction based upon iterative computer optimization routines, and (3) a combination of (1) and (2) where as many elements as possible are quickly identified, providing constraints to the software optimization routine that serves as the validity check.

All of the above methods can be applied to the standard HEMT small-circuit model, the hybrid-π circuit topology [14]. The small-signal elements in Fig. 5 are broken down into the intrinsic and extrinsic elements. The intrinsic elements are the transconductance, g_m; output conductance, g_{ds}; gate-source capacitance, C_{gs}; gate-drain capacitance, C_{gd}; drain-source capacitance, C_{ds}; gate-source resistance, R_{gs}; and delay time, τ. These elements are bias dependent and important to the understanding of device behavior. The extrinsic elements are independent of bias and include the three terminal inductances, L_g, L_d, and L_s, the contact resistances for the three terminals, R_g, R_d, and R_s, and the parasitic pad capacitances, C_{pg} and C_{pd}.

The simplest and most straight-forward method is the complete parameter extraction method. It has been shown that, with a sequence of microwave and dc measurements, each term can be uniquely determined [13]. A so-called shell technique can be applied to remove the inductances, the pad parasitics, and the contact resistances. For this technique, the S-parameters of the device are measured for a variety of drain-to-source voltage conditions. By using the simplifying assumptions that $\omega^2 C_{gs}^2 R_{gs}^2 < 0.01$ and that $\omega\tau << 1$, one can determine the parasitic elements uniquely, leaving only the intrinsic circuit to be determined. The drawbacks to this method are that several measurements must be made under different bias conditions and simplifying assumptions must be made, increasing the uncertainty of the extracted parameters.

The second method of extraction is to simply fit the measured S-parameters to the equivalent circuit by iteratively solving for the individual elements. The disadvantage to this technique is that, with such a large parameter space, it is very difficult to uniquely identify each element. This frequently produces unrealistic values for a number of the circuit elements.

The most desirable and accurate method is to apply the techniques from the complete parameter extraction method coupled with small-signal circuit optimization routines that serve as a validity check. The important parasitics are estimated by measuring a simple test structure and by independent dc measurements. Although a test structure for the parasitic elements was not available, this was the method used for this work, and it is described in more detail in the next section.

V. Measurement Results

For this device study, a passivated, planar doped pseudomorphic 0.25 × 75 μm (gate length × width) HEMT manufactured by GE was selected. This structure is grown on a semi-insulating GaAs wafer. To inhibit impurity diffusion into the active InGaAs region, the first layer grown is a 1-μm thick GaAs buffer layer. A spacer layer of undoped AlGaAs 45 $\AA$ thick is grown between the doping and the active region to reduce dopant donor ion/conduction electron interactions. The silicon dopant concentration

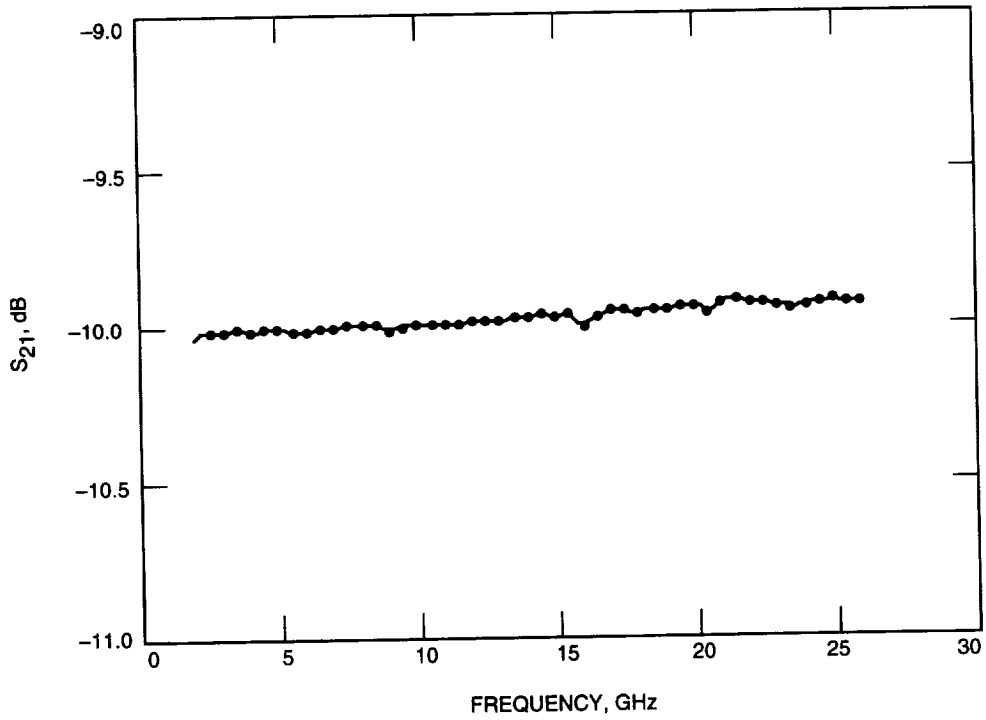

Fig. 4. Transmission through a 10-dB attenuator at a physical temperature of 20 K using LRM calibration.

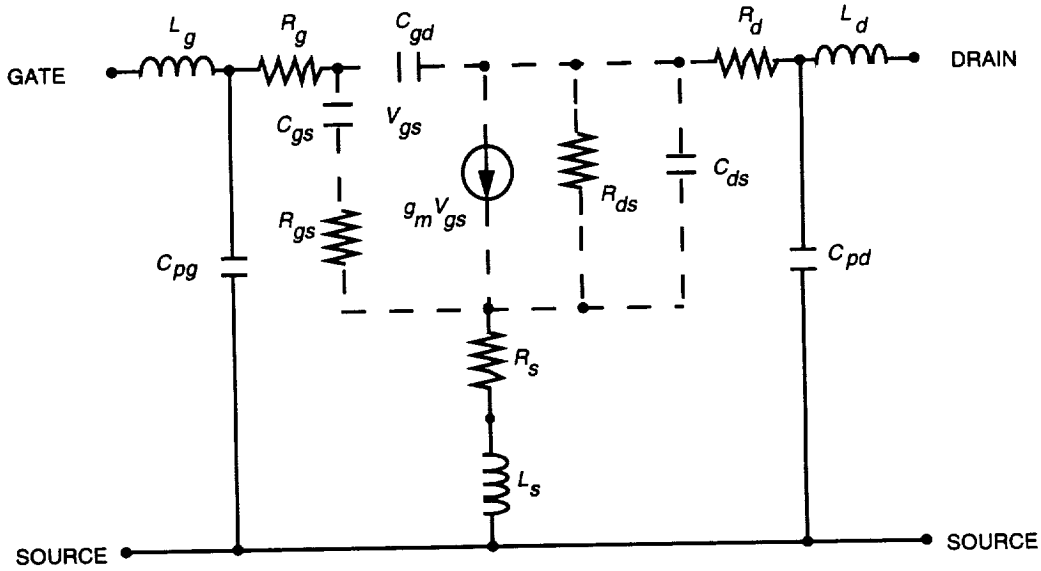

Fig. 5. Small-signal circuit diagram of PHEMT showing intrinsic and extrinsic elements.

of 3×10^{12} atoms/cc is grown in a single plane approximately 3 Å thick. Heavily doped AlGaAs and GaAs layers 400 and 350 Å thick, respectively, are grown to provide ohmic contacts. A schematic representation of this heterostructure is shown in Fig. 6. This layered structure produces a conduction band discontinuity that forms a triangular one-dimensional quantum well at the AlGaAs/InGaAs heterojunction.

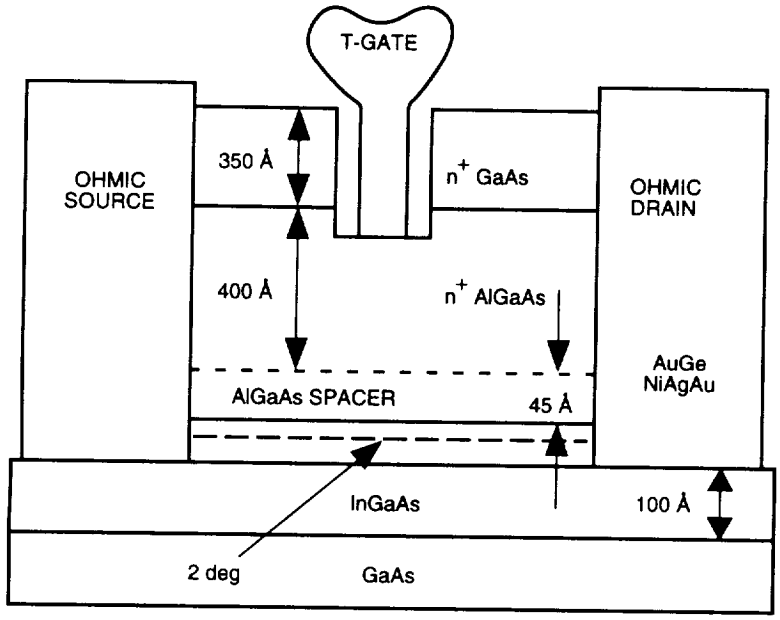

Fig. 6. Schematic representation of the PHEMT.

The noise and scattering parameters were measured for a variety of temperatures and bias conditions over a broad frequency span. Scattering parameters were measured from 1 to 25 GHz, while noise parameter measurements were attempted from 2 to 18 GHz for the same bias and temperature conditions. For all of the experimental conditions, all the S-parameters were measured with an error of less than 2 percent. A polar plot comparing S_{21} at two physical temperatures, 16 and 300 K, is shown in Fig. 7. Unfortunately, all four noise parameters could not be reliably measured for the physical temperature and frequency spans of interest. At room temperature, all four noise parameters were obtained. A plot from 2 to 18 GHz showing the scatter in the measured optimum source impedance (real part = $RE[\Gamma_{opt}]$; imaginary part = $IM[\Gamma_{opt}]$) at room temperature is displayed in Fig. 8. At cryogenic temperatures, however (as discussed in Section III), because of the lossy input and long electrical distance of the impedance generator from the device input, only the minimum noise temperature was reliably determined. In fact, at the lower frequencies (2 to 8 GHz) and physical temperatures (11 to 39 K) the percentage error in the noise parameters was too large ($\approx$ 80 percent) to be useful. For frequencies above 8 GHz, the percentage error in the minimum noise temperature was determined to be less than 25 percent. The resulting measurements were then fit to a straight line. The fitting error varied from 6 to 11 percent. Figure 9 shows a plot of the measured minimum noise temperature as a function of percentage drain to source saturation current at 18 GHz at five physical temperatures, from 16 to 300 K. Over this temperature range, the rms error in the minimum noise temperature varied from $\pm$ 12 K to $\pm$ 6 K.

For this study, the device small-signal circuit elements were determined using two sets of measured S-parameters and with the measurement probes calibrated with LRM standards at the physical temperatures of interest. The first set, or cold FET ($V_{ds} = 0$), measurements determine the bias independent extrinsic elements, while the biased device measurements are used to determine the intrinsic elements. All of the extracted elements for the different physical temperatures and bias settings are displayed in Table 1 along with $R_t(R_s + R_g + R_{gs})$, estimated T_d, and the calculated T_{min} per unit frequency.

To determine the uniqueness of the extracted intrinsic circuit elements, the extraction algorithm was run several times and the results compared. For this test, the extrinsic elements were kept constant and initial starting values for a variety of the intrinsic elements were purposely chosen to be up to a factor of two larger or smaller than the final value. For all the cases tried, the worst variation of any of the

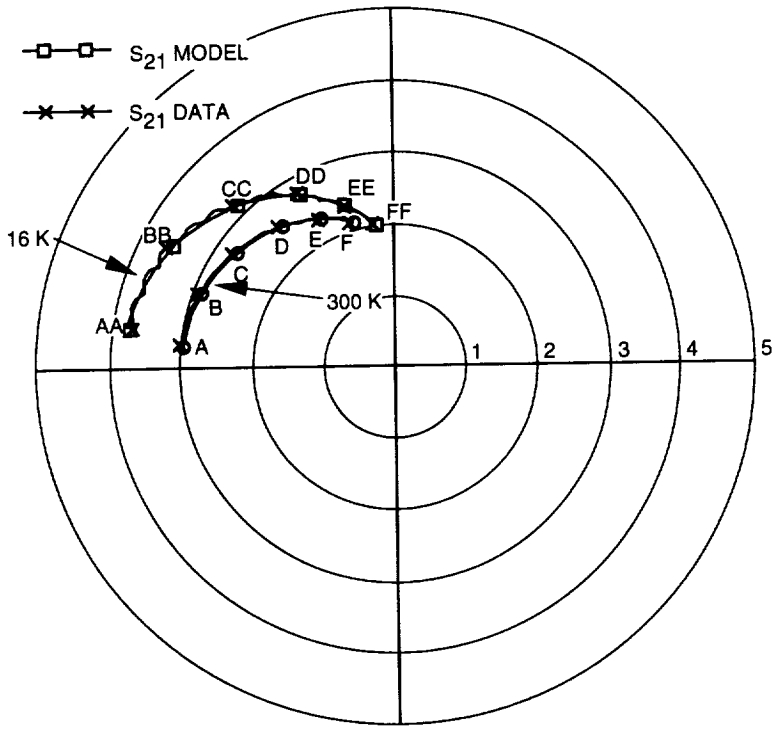

Fig. 7. A comparison of S_{21} for the PHEMT, at 16 and 300 K (frequency: 2 to 25 GHz).

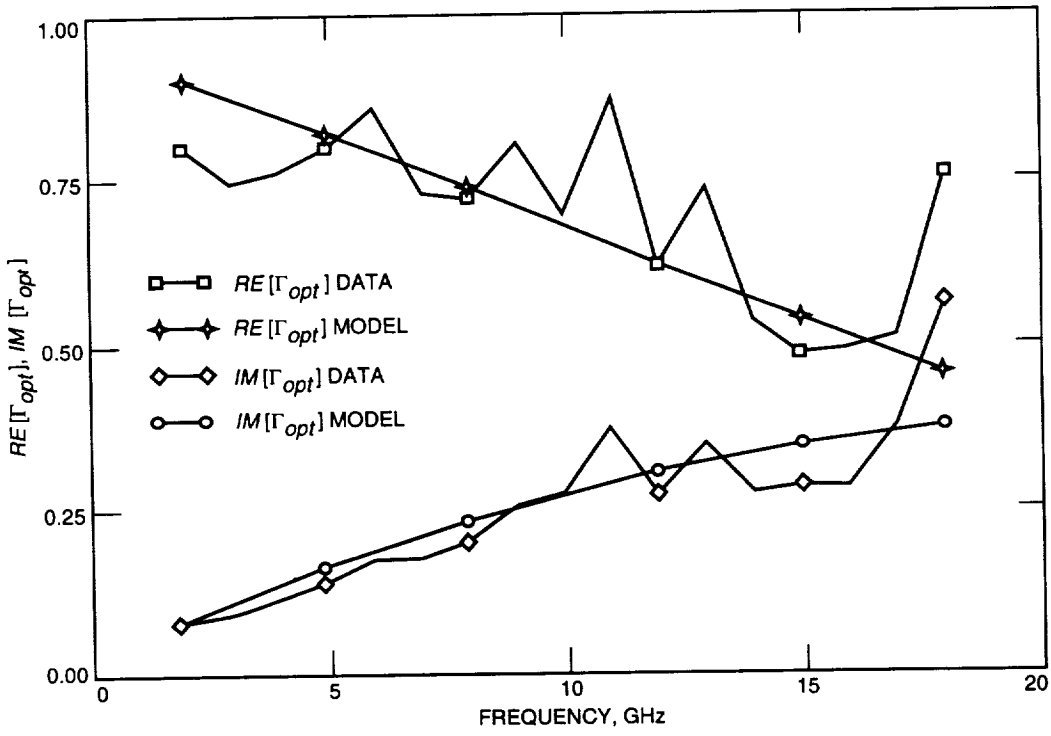

Fig. 8. Scatter in the measured optimum source impedance at room temperature (2 to 18 GHz).

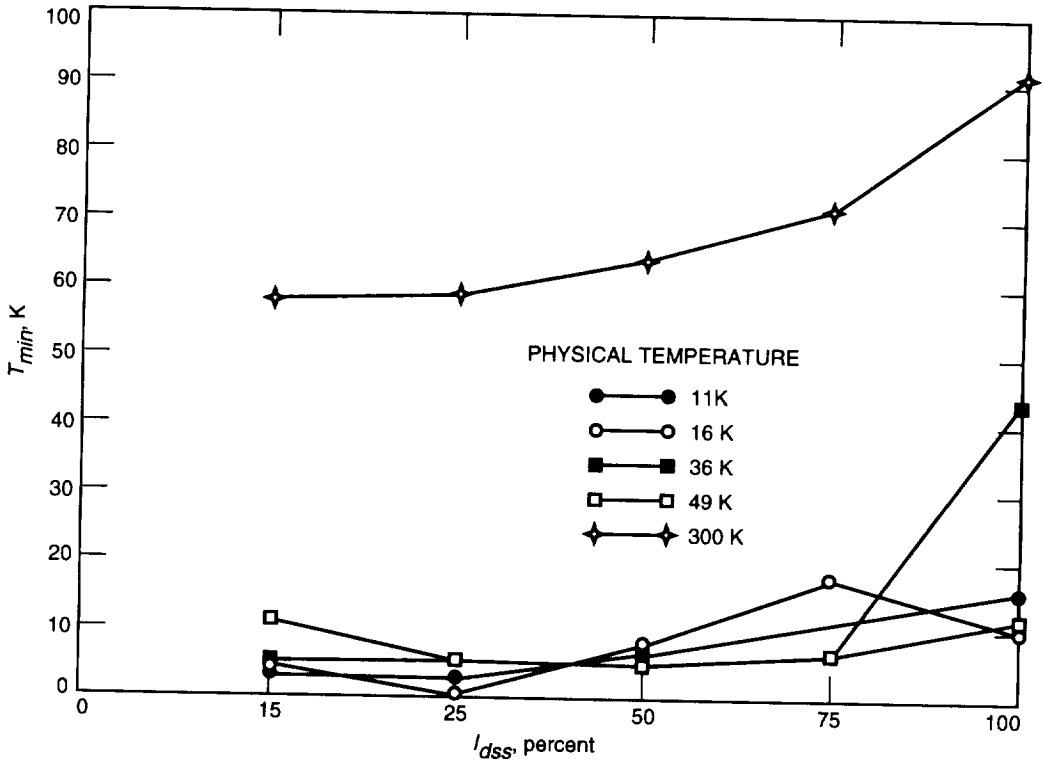

Fig. 9. Measured noise temperature at 18 GHz at several temperatures.

intrinsic elements was no more than 2 percent. Additionally, S-parameters for a biased device were used to simultaneously extract both intrinsic and extrinsic element values. In this case, for the same value of fitting error, some of the element values varied as much as 110 percent for R_{gs} or as little as 5 percent for C_{gs}.

VI. Analysis and Discussion

The pioneering work of Weinreb and Pospieszalski [15,16] has led to the development of HEMT-based LNAs that are the lowest noise transistor circuits produced to date. These impressive results have been achieved without the benefit of cryogenic, broadband noise measurements. Pospieszalski's method relies on dc cryogenic measurements (g_m and R_{ds}), manufacturers or measured room-temperature broadband S-parameter data (remaining circuit elements), and a single-frequency cryogenic noise-parameter measurement (T_d and T_g) to determine all of the circuit parameters for his empirical noise model.

For the Pospieszalski noise model [17], the measured noise parameters are required to determine T_d, the equivalent drain temperature associated with g_{ds}, and the equivalent gate temperature T_g associated with R_{gs} and as an additional check on the intrinsic element values. Pospieszalski [18] found that, for a variety of different HEMT and FET devices, T_g was equal to the ambient temperature for I_{ds} less than 20 mA. On the other hand, T_d is strongly dependent on I_{ds} and, within measurement error, a single function may describe its dependence for all devices. (At room temperature, using on-wafer noise and scattering parameters from 4 to 18 GHz, Pospieszalski used measured and modeled values for the intrinsic R_{opt} and T_{min} using a least-squares fit to arrive at values of T_d and T_g.)

Ideally, for low-noise device studies and circuit modeling, it is preferable to have both broadband measured noise and scattering parameters. Since only the measured minimum noise temperatures were obtained, only the predicted and measured noise temperatures as a function of drain currents (I_{ds}) at

Table 1. Extracted elements for the different physical temperatures and bias settings.

I_{dss}, %	I_{dss}, mA	L_d, pH	L_g, pH	L_s, pH	R_d, Ω	R_g, Ω	R_s, Ω	C_{ds}, fF	C_{gd}, fF	C_{gs}, fF	G_m, ms	R_{ds}, Ω	R_{gs}, Ω	R_t Ω	T_d, K	T_{min}/f, K/GHz
T_{phys} = 11 K																
15	2.9	4	15	4	5.0	3.8	1.00	17.20	22.90	76.50	39.70	576.70	1.00	5.80	234	0.123
25	4.7	4	15	4	4.6	3.8	1.00	17.40	22.20	84.30	50.30	450.00	1.00	5.80	373	0.153
50	9.6	4	15	4	4.7	3.5	1.00	17.30	21.60	91.40	65.00	370.00	1.00	5.50	750	0.196
75	14.9	4	15	4	6.7	3.0	1.00	18.80	21.20	92.20	72.00	344.20	0.70	4.70	1158	0.212
100	18.7	4	15	4	6.0	3.0	1.00	19.00	19.72	103.00	72.00	331.80	1.50	5.50	1451	0.292
T_{phys} = 16 K																
15	2.4	4	15	4	6.0	3.0	2.00	18.80	31.10	68.60	36.25	589.00	2.00	7.00	201	0.147
25	3.9	4	15	4	6.0	3.0	1.00	17.00	31.00	71.00	45.30	480.00	2.00	6.00	316	0.157
50	8.4	4	15	4	6.0	2.0	1.00	17.90	30.40	78.70	60.90	368.00	2.00	5.00	663	0.195
75	12.7	4	15	4	6.0	3.0	1.00	15.70	30.10	80.80	68.50	344.80	2.00	6.00	994	0.247
100	16.4	4	15	4	6.0	3.0	2.30	17.60	25.50	123.60	67.00	303.00	2.00	7.30	1279	0.515
T_{phys} = 36 K																
15	2.5	4	15	4	6.0	3.0	2.27	22.25	24.77	72.19	35.07	625.75	11.21	16.48	229	0.381
25	4.1	4	15	4	6.0	3.0	2.27	21.42	24.41	80.78	47.44	469.76	7.92	13.19	352	0.403
50	8.3	4	15	4	6.0	3.0	2.27	21.88	23.39	92.24	64.56	352.77	6.00	11.27	675	0.500
75	12.5	4	15	4	6.0	3.0	2.27	15.47	29.67	90.21	74.60	298.41	5.50	10.77	999	0.547
100	16.4	4	15	4	6.0	3.0	2.27	16.91	24.56	133.61	66.91	303.99	5.50	10.77	1299	1.021
T_{phys} = 49 K																
15	2.2	4	15	4	6.0	3.0	2.27	21.83	24.93	72.19	35.42	526.80	10.88	16.15	218	0.464
25	3.7	4	15	4	6.0	3.0	2.27	21.51	24.39	71.92	47.40	468.31	7.20	12.47	334	0.398
50	7.5	4	15	4	6.0	3.0	2.27	21.88	23.39	92.24	64.56	352.77	6.00	11.27	627	0.562
75	11.1	4	15	4	6.0	3.0	2.27	20.65	23.06	96.51	72.77	324.14	6.00	11.27	904	0.654
100	15.8	4	15	4	6.0	3.0	2.27	21.69	17.45	137.63	66.24	315.41	6.00	11.27	1266	1.229
T_{phys} = 300 K																
15	2.7	4	15	4	6.0	3.1	3.40	17.10	19.50	69.60	28.13	798.00	2.00	8.50	508	1.253
25	4.6	4	15	4	6.0	3.0	4.90	19.30	18.33	83.60	40.36	560.00	2.00	9.90	654	1.533
50	9.1	4	15	4	6.0	1.5	3.40	18.70	18.02	90.00	51.00	464.90	2.00	6.90	1001	1.480
75	13.8	4	15	4	6.0	3.0	3.50	18.40	17.41	96.60	57.90	417.70	2.00	8.50	1363	1.912
100	18.4	4	15	4	6.0	1.96	3.70	18.24	17.05	101.60	60.40	398.30	2.00	7.66	1717	2.104

18 GHz for a variety of different temperatures are compared. The predicted minimum noise temperature is calculated using Pospieszalski's expression,

$$T_{min} = \frac{2\pi f C_{gs}\sqrt{g_{ds}R_t T_g T_d}}{g_m}$$

for the minimum noise temperature. The small-signal circuit elements are those extracted from the measured S-parameters, while T_g is the device physical temperature and T_d is estimated from the results in [18].

Figure 10 shows a comparison of the room temperature results as a function of percentage of drain saturation current. The measured minimum noise temperature is more than a factor of two larger than the predicted values. This discrepancy is probably associated with an unrealistic extracted value for R_t. The extracted value for R_t at room temperature is approximately the same as the value at 11 and 16 K and 50 percent smaller than the 36- and 49-K extract value (see Table 1 and Fig. 11). The room temperature, R_t, should have been 2 to 4 times the cryogenic value. However, at cryogenic temperatures for low drain-current values, the measured and modeled results agree within the measurement uncertainties (see Fig. 12).

For single-frequency measurements at 18 GHz, the worst-case errors for the measured minimum noise temperature are ± 25 K and ± 15 K for the calculated model values. That the cryogenic results agree is possibly fortuitous. However, that there is agreement indicates that a closer examination with a more accurate and reliable method of cryogenic noise parameter measurement and small-signal element extraction technique is absolutely necessary.

Three of the four intrinsic circuit elements, g_m, g_{ds}, and C_{gs}, that determine T_{min} behaved as expected. The transconductance, g_m, and the output conductance, g_{ds}, were observed to show significant increases upon cooling and increasing drain current (see Figs. 13 and 14). The C_{gs} shown in Fig. 15 is relatively constant with temperature but increases linearly with increasing bias while, on the other hand, the gate resistance, R_{gs}, flip-flops, increasing in resistance as the temperature is lowered toward 36 K but dropping to its room temperature value at 16 K and half that value at 11 K (see Fig. 11). In addition, for high drain-current values, the resistance appears to be independent of drain current value. Clearly, more accurate noise-parameter measurements at these cryogenic temperatures will significantly increase our knowledge of the temperature behavior of the parameters that determine cryogenic noise performance of HEMTs.

VII. Conclusion

The feasibility of cryogenic, broadband on-wafer scattering parameter measurements has been demonstrated. It was also shown that a commercial noise-parameter measurement system is inadequate for cryogenic applications. Although some useful cryogenic noise temperature data were obtained, it was not of sufficient density or accuracy for a systematic device study. Systematic studies are necessary to develop device technologies for future applications and to properly select, develop, and design high-performance cryogenic LNAs.

The development of a cryogenic probe tip integrated with a cryogenic noise and impedance generator capable of performing both scattering and noise parameter measurements will circumvent the limitations posed by the current characterization techniques. This type of probe will allow nondestructive characterization of devices and circuits while still in wafer form. This measurement technique will provide significant cost savings by improving accuracy and design methodology and by reducing test verification costs. Once operational, such a system will be beneficial in studying HEMT LNAs as well as hybrid semiconductor/superconductor circuits.

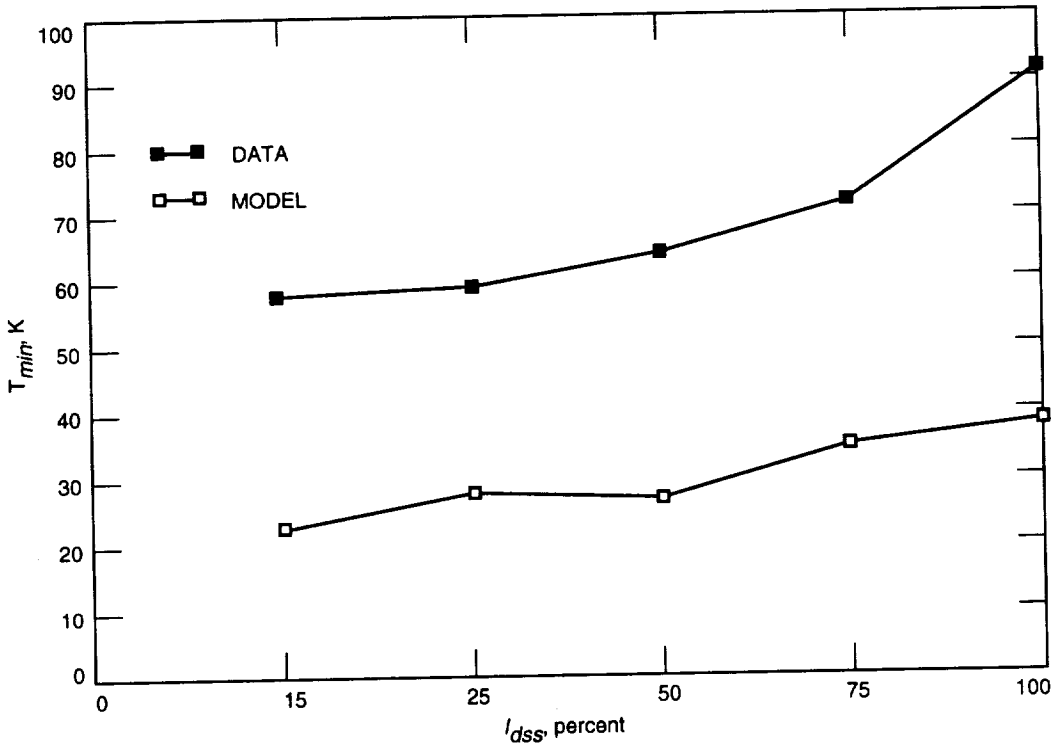

Fig. 10. Measured data versus model at a 300-K physical temperature at 18 GHz.

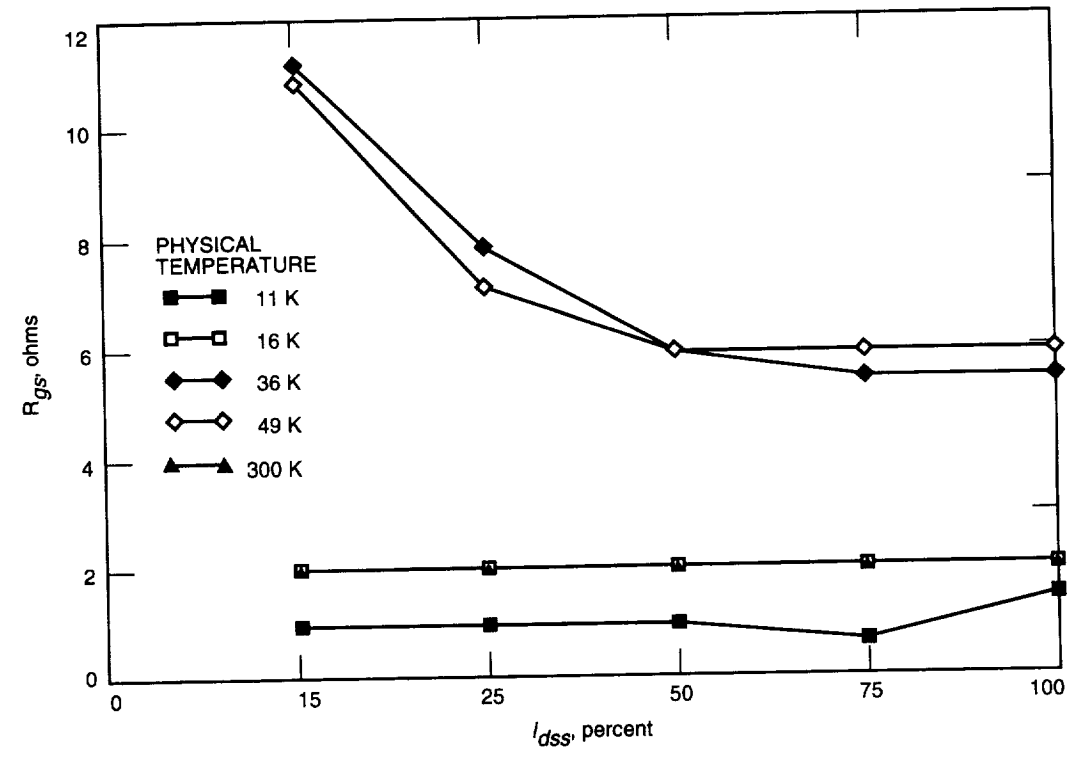

Fig. 11. R_{gs} at several temperatures.

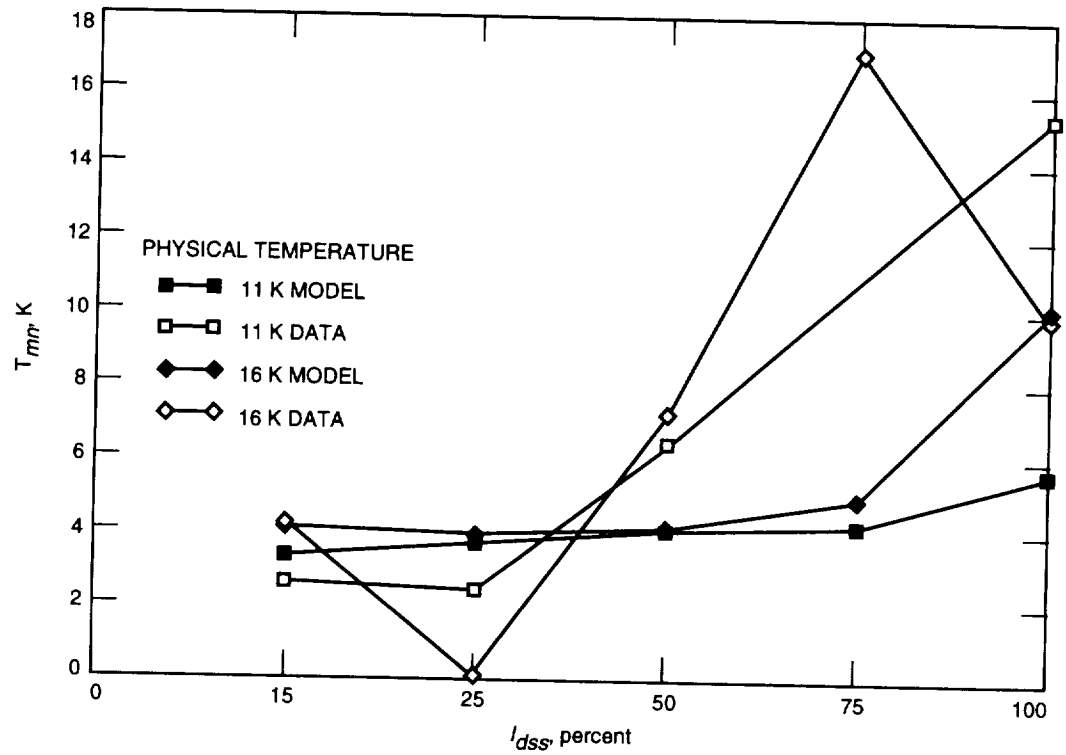

Fig. 12. Model and measured data at 18 GHz; 11 and 16 K.

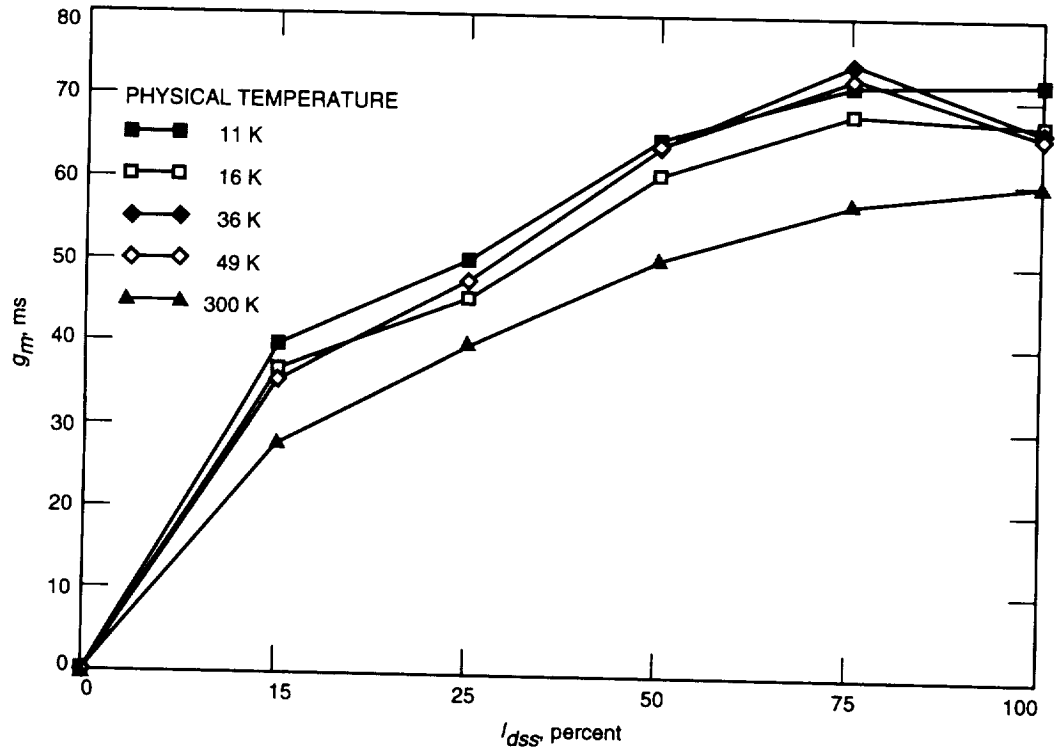

Fig. 13. G_m for several temperatures.

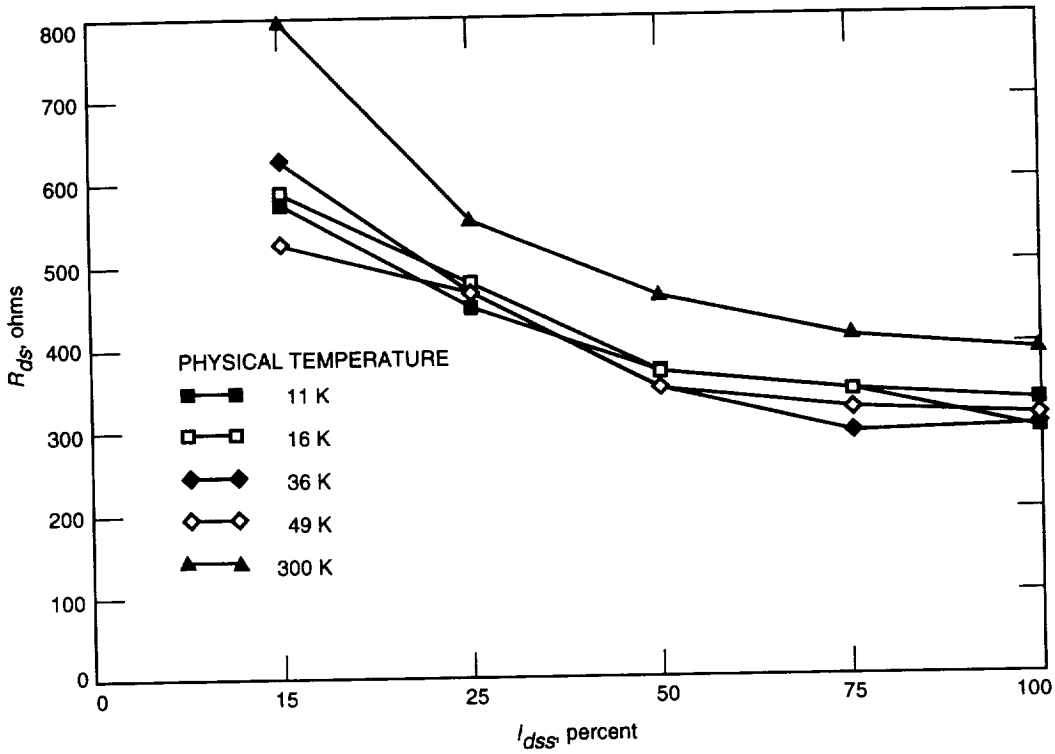

Fig. 14. R_{ds} at several temperatures.

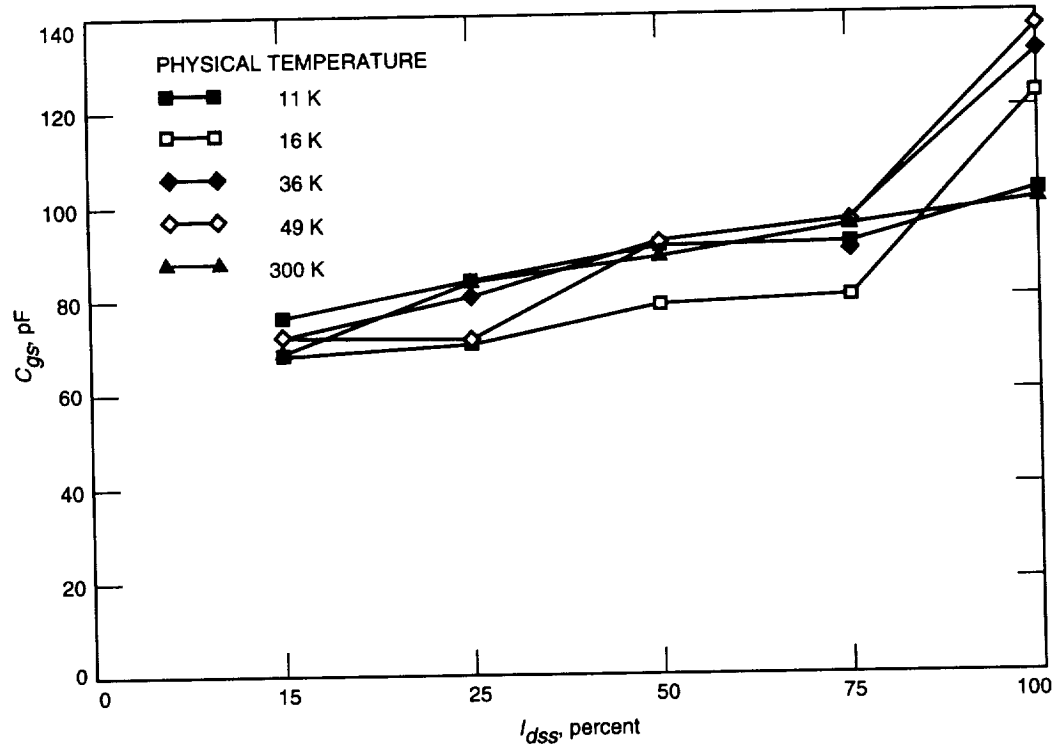

Fig. 15. C_{gs}, at several temperatures.

JPL's experience with HEMT-based LNAs is that they are easier to operate and less costly than masers. Although masers provide the lowest noise temperature, HEMTs can, in principle, perform as well as masers. The development of an integrated probe for cryogenic, broadband scattering and noise-parameter measurements will significantly bolster the existing JPL HEMT program to continue the development of HEMT devices and LNAs with maser-like noise temperatures. The advent of super–low noise HEMT devices will lead to greater frequency coverage and economical cryogenic, single- and multiple-element feed systems for routine telemetry and radio navigation.

References

[1] C. A. Liechti and R. B. Larrick, "Performance of GaAs MESFET's at Low Temperatures," *IEEE Trans. Microwave Theory Tech.*, vol. MTT-24, pp. 365–370, June 1976.

[2] W. Brockerhoff, H. Meschede, W. Prost, K. Heime, G. Weimann, and W. Schapp, "RF Measurements and Characterization of Heterostructure Field-Effect Transistors at Low Temperatures," *IEEE Trans. Microwave Theory Tech.*, vol. 37, pp. 1380–1388, September 1989.

[3] S. T. Fu, M. Das, P. C. Chao, K. Duh, P. Ho, and J. Ballingall, *Workshop on Low Temperature Semiconductor Electronics*, p. 19, 1989.

[4] J. Kolodzey, H. Laskar, S. Boor, S. Reis, A. Ketterson, I. Adesida, D. Sivco, R. Fischer, and A. Y. Cho, "Cryogenic Temperature Performance of Modulation Doped Field Effect Transistors," *Electon. Lett.*, vol. 25, pp. 777–778, 1988.

[5] R. Lai, P. K. Bhattacharya, D. Yang, T. L. Brock, A. A. Alterovitz, and A. N. Downey, *IEEE Trans. on Elec. Dev.*, vol. 39, p. 2206, 1992.

[6] J. W. Smuk, M. G. Stubbs, and J. S. Wight, "Vector Measurements of Microwave Devices at Cryogenic Temperatures," *1989 IEEE MTT-S International Microwave Symposium*, New York: The Institute of Electrical and Electronic Engineers, Inc., pp. 1195–1198, June 1989.

[7] S. Weinreb, "Low-Noise Cooled GASFET Amplifiers," *IEEE Trans. Microwave Theory Tech.*, vol. MTT-28, pp. 1041–1054, October 1980.

[8] J. Laskar and J. Kolodzey, "Vacuum Cryogenic High Frequency Probe Station," *J. Vac. Sci. Technol. B*, vol. 8, pp. 1161–1165, September–October 1990.

[9] J. Laskar and M. Feng, "An On-Wafer Cryogenic Microwave Probing System for Advanced Transistor and Superconductor Applications," *Microwave Journal*, vol. 36, pp. 104–114, February 1993.

[10] *Cascade Microtech Model 42D User's Manual*, Cascade Microtech, Beaverton, Oregon, 1987.

[11] H. Meschde, R. Reuter, J. Albers, J. Kraus, D. Peters, W. Brockerhoff, F. Tegude, M. Bode, J. Schubert, and W. Zander, "On-Wafer Microwave Measurement Setup for Investigations on HEMT's and High Tc Superconductors at Cryogenic Temperatures Down to 20 K," *IEEE Trans. Microwave Theory Tech.*, vol. 40, pp. 2325–2331, December 1992.

[12] Y. Kwark, P. Solomon, and D. Tulipe, *Proc. of IEEE/Cornell Univ. Conf. on Advanced Concepts in High Speed Semic. Dev. and Ckts.*, New York, p. 208, 1989.

[13] G. Dambrine, A. Cappy, F. Heliodor, and E. Playez, "A New Method for Determining the FET Small-Signal Equivalent Circuit," *IEEE Trans. Microwave Theory Tech.*, vol. 36, pp. 1151–1159, July 1988.

[14] C. A. Liechti, "Microwave Field-Effect Transistors—1976," *IEEE Trans. Microwave Theory Tech.*, vol. 24, pp. 279–300, June 1976.

[15] S. Weinreb, R. Harris, and M. Rothman, "Millimeter-Wave Noise Parameters of High Performance HEMT's at 300 K and 17 K," *1989 IEEE MTT-S International Microwave Symposium Digest*, New York: The Institute of Electrical and Electronic Engineers, Inc., pp. 813–816, June 1989.

[16] M. W. Pospieszalski, "Cryogenically Cooled HFET Amplifiers and Receivers: State-of-the-Art and Future Trends," *1992 IEEE MTT-S International Microwave Symposium Digest*, New York: The Institute of Electrical and Electronic Engineers, Inc., pp. 1369–1372, June 1992.

[17] M. W. Pospieszalski, "Modeling of Noise Parameters of MESFET's and MODFET's and Their Frequency and Temperature Dependence," *IEEE Trans. Microwave Theory and Tech.*, vol. MTT-37, pp. 1340-1350, September 1989.

[18] M. W. Pospieszalski and A. C. Niedwiecki, "FET Noise Model and On-Wafer Measurement of Noise Parameters," *1991 IEEE MTT-S International Microwave Symposium Digest*, New York: The Institute of Electrical and Electronic Engineers, Inc., pp. 1117–1122, June 1991.